Effect of Different Subsectional Basis and Testing Function in the Method of Moments for the Scattering from Two Dimensional Dielectric Scatterers

[1*]Ng Tze Wei, [1,2]Zulkifly Abbas and [2]Nurul Huda Osman

[1]*Institute for Mathematical Research, Universiti Putra Malaysia, 43400 UPM Serdang, Selangor, Malaysia*

[2]*Department of Physics, Faculty of Science, Universiti Putra Malaysia, 43400 UPM Serdang, Selangor, Malaysia*

E-mail:ngwei302@gmail.com

*Corresponding author

ABSTRACT

Different integral equations are reduced to a system of linear equations via method of moments (MoM) where the different basis and testing function utilised are sinusoid/pulse, sinusoid/sinusoid, sinusoid/triangle, triangle/pulse, triangle/sinusoid and triangle/triangle method. A hollow/layered dielectric cylinder has been taken as a representative case study. Comparison is made on the convergence and accuracy due to different testing function where the mean relative error is investigated numerically to show the essential differences of different basis and testing function in the MoM using different implementation techniques and different boundary conditions. The Gauss quadrature and staircase approximation technique is used in calculating the impedance matrix elements. The different boundary conditions utilised is the exact and impedance boundary condition. Numerical results points out to the need to investigate the performance of other basis and testing functions for dielectric scatterers.

Keywords: Method of moments, surface integral equation, numerical analysis, error analysis

1. INTRODUCTION

Different numerical techniques have been applied in electromagnetic problems such as the MoM for the radiation, scattering and

many other applications where numerical results are verified using exact solutions, measured data, solution obtained from other techniques providing the user confidence regarding the accuracy of the numerical solution (Davis *et al.* (2005)). Surface integral equations were developed to allow treatment of 2 dimensional scatterers to overcome memory size limitation needed for computer code implementation (Beker *et al.* (1990)). The continuous linear operator is projected onto finite dimensional subspaces defined by the basis and testing functions when the method of moments (MoM) is used to discretise the continuous linear equation into a matrix system to produce an approximate solution (Peterson (1998)). The choice of basis and testing functions plays a role in the accuracy and convergence of results where the theoretical convergence rates of the current error and scattering error in transverse magnetic (TM) and transverse electric (TE) scattering by a circular conducting cylinder is investigated (Davis *et al.* (2004)) for different expansion and testing sets. However, the effect of permittivity of dielectric object towards the convergence and accuracy of the numerical solution is not taken into account. Usually one would resort to increase the matrix size in the MoM to minimize the error in numerical computations so that this can increase the users' confidence of the numerical solution. Consequently, this would result in higher computer storage requirement of the impedance matrix elements and the computation time would also increase. This effect becomes worse for large size dielectric object because the matrix size required would be very high to achieve an accurate solution.

The MoM results in fully populated matrices (Jin (2010)) and therefore the computing time and computer storage requirement is greatly increase when the matrix size is increased and therefore this is not always desirable. When the MoM impedance matrix size has to be reduced in order to save the computer storage requirements and computation time, different basis and testing function can result in different amount of error contamination at different mesh density when dealing with dielectric scatterers. Different implementations can give different convergence rate and different memory requirements even though the numerical technique used is the same (Jin (2010)) and this may depend on the basis and testing function utilised. Therefore, a comparative study on the effect of different subsectional testing function towards the variation of error with samples/wavelength for dielectric scatterers is worthwhile because the testing function that give a more acceptable result using a smaller impedance matrix size or faster convergence can be selected to save computer storage requirements and computation time.

In this paper, the different basis and testing function considered for numerical solution is the triangle/pulse (TP), triangle/triangle (TT), triangle/sinusoid (TS), sinusoid/pulse (SP), sinusoid/triangle (ST), and sinusoid/sinusoid (SS). Triangle/sinusoid refers to triangle basis sinusoid testing. These basis and testing function are selected as the coefficients of the basis function remains finite and well defined for any location of the basis and testing function throughout the domain (Peterson (1998)).

The different integral equation formulation considered in this paper is the electric field integral equation (EFIE), magnetic field integral equation (MFIE), Poggio-Muller-Chu-Harrington-Wu integral equation (PMCHW) and Muller integral equation (Kishk (1991)). Two different numerical implementation techniques are considered in computing the impedance matrix elements which is the Gauss quadrature and staircase approximation technique.

2. THEORY

The electric and magnetic fields generated by the surface electric currents, $\vec{J}$ and surface magnetic currents, $\overline{M}$ are as follows (Kishk (1991)).

$$\vec{E}^{s}(\vec{J}) = -j\omega\vec{A}(\vec{J}) - j\frac{1}{\omega\mu\varepsilon}\nabla\nabla\cdot\vec{A}(\vec{J}) . \tag{1}$$

$$\vec{E}^{s}(\overline{M}) = -\frac{1}{\varepsilon}\nabla\times\overline{F}(\overline{M}) . \tag{2}$$

$$\overline{H}^{s}(\vec{J}) = \frac{1}{\mu}\nabla\times\vec{A}(\vec{J}) . \tag{3}$$

$$\overline{H}^{s}(\overline{M}) = -j\omega\overline{F}(\overline{M}) - j\frac{1}{\omega\mu\varepsilon}\nabla\nabla\cdot\overline{F}(\overline{M}) . \tag{4}$$

$$\vec{A}(\vec{J}) = \mu\int\vec{J}(\vec{\rho}\,')G(\vec{\rho},\vec{\rho}\,')d\vec{\rho}\,' . \tag{5}$$

$$\overline{F}(\overline{M}) = \varepsilon\int\overline{M}(\vec{\rho}\,')G(\vec{\rho},\vec{\rho}\,')d\vec{\rho}\,' . \tag{6}$$

$$G(\vec{\rho},\vec{\rho}\,') = (\frac{1}{j4})\cdot H_{0}^{(2)}(k\,|\,\vec{\rho}-\vec{\rho}\,'|) . \tag{7}$$

$$k = \omega \sqrt{\mu\varepsilon} \; . \tag{8}$$

$$\omega = 2\pi f \tag{9}$$

$G(\overline{\rho},\overline{\rho}')$ is the 2 dimensional Green's function and $\overline{\rho}'$ and $\overline{\rho}$ are the source and the observation points respectively. In this manuscript, the time convention $e^{j\omega t}$ is selected. μ is the permeability whereas ε is the permittivity and f is the frequency. According to the surface equivalence principle, the boundaries of region V_i with permittivity ε_{ri} and permeability μ_{ri} are replaced by electric currents for conducting surfaces and equivalent electric and equivalent magnetic currents for dielectric boundaries to obtain the fields in region V_i (Kishk (1991)). To ensure the continuity of the tangential component of the fields dielectric interface, the surface currents appearing on the opposite sides of the interface is taken to be of the same magnitude and in the opposite direction (Kishk (1991)). The boundary conditions on conducting and dielectric surfaces is

$$\hat{n}\times\overline{E_d}=0 \;\; \text{on} \;\; S_{cd}. \tag{10}$$

$$\hat{n}\times\overline{E_e}=0 \;\; \text{on} \;\; S_{cf}. \tag{11}$$

$$\hat{n}\times\overline{E_d}=\hat{n}\times\overline{E_e} \;\; \text{on} \;\; S_{df}. \tag{12}$$

$$\hat{n}\times\overline{H_d}=\hat{n}\times\overline{H_e} \;\; \text{on} \;\; S_{df}. \tag{13}$$

S_{cd} is the interface between conducting and dielectric regions. S_{cf} is the interface between conducting and free space region. S_{df} is the interface between dielectric and free space region. Equation (12) and (13) is used as the exact boundary condition (EBC) that can be replaced by the impedance boundary condition (IBC) which is given by (Kishk (1991))

$$\hat{n}\times\vec{E_1}\times\hat{n}=\eta_1\eta_0(\hat{n}\times\vec{H_1}) \tag{14}$$

$$\eta_1=\sqrt{\frac{\mu_r}{\varepsilon_r}} \tag{15}$$

For the details regarding the derivation of the surface integral equation, one can easily refer to (Beker (1990)) and they will not be repeated here. The combined field integral equation is utilised to avoid

spurious solution due to the interior resonance problem on closed
conducting and impedance surfaces (Huddleston *et al.* (1986)), (Kishk
(1991)).

The different surface integral equations are reduced to matrix
system involving unknown surface currents using the MoM and the general
matrix takes the form $[V_m] = [Z_{mn}][I_n]$ where $[Z_{mn}]$ is the square impedance
matrix, $[I_n]$ is the column matrix for the unknown expansion coefficients of
the surface currents respectively and $[V_m]$ is the excitation column matrix
(Kishk (1991)). By solving the system matrix, the induced currents on all
the interfaces can be determined. The generic integrals resulted from the
MoM are as follows (Gibson (2007)).

$$\int f_m(\overline{\rho})\hat{z} \cdot \overline{X}(K\hat{z})d\overline{\rho}$$
$$= \int f_m(\overline{\rho}) \cdot \int K(\overline{\rho}')G(\overline{\rho},\overline{\rho}')d\overline{\rho}'d\overline{\rho}. \tag{16}$$

$$\int f_m(\overline{\rho})\hat{t}(\overline{\rho}) \cdot \overline{X}(K\hat{t})d\overline{\rho}$$
$$= \int f_m(\overline{\rho}')\hat{t}(\overline{\rho}')G(\overline{\rho},\overline{\rho}')d\overline{\rho}'d\overline{\rho}. \tag{17}$$

$$\int f_m(\overline{\rho})\hat{t}(\overline{\rho}) \cdot \nabla\nabla \cdot \overline{X}(K\hat{t})d\overline{\rho}$$
$$= \int f_m(\overline{\rho})\hat{t}(\overline{\rho}) \cdot \nabla\nabla \cdot \int K(\overline{\rho}')\hat{t}(\overline{\rho}')G(\overline{\rho},\overline{\rho}')d\overline{\rho}'d\overline{\rho}. \tag{18}$$

$$\int f_m(\overline{\rho})\hat{z} \cdot \nabla \times \overline{X}(K\hat{t})d\overline{\rho}$$
$$= \int f_m(\overline{\rho}) \cdot \int K(\overline{\rho}')(\hat{z} \times \hat{t}(\overline{\rho}')) \cdot \nabla'G(\overline{\rho},\overline{\rho}')d\overline{\rho}'d\overline{\rho}. \tag{19}$$

$$\int f_m(\overline{\rho})\hat{t}(\overline{\rho}) \cdot \nabla \times \overline{X}(K\hat{z})d\overline{\rho}$$
$$= \int f_m(\overline{\rho}) \cdot \int K(\overline{\rho}')(\hat{t}(\overline{\rho}') \times \hat{z} \cdot \nabla'G(\overline{\rho},\overline{\rho}')d\overline{\rho}'. \tag{20}$$

where $\overline{X} = \overline{A}$ or $\overline{F}$ and $\overline{K} = \overline{J}$ or $\overline{M}$.

The singularity of the generic integral (19) and (20) is extracted
using Cauchy principal value integration before evaluating the integral
regardless of the basis and testing function employed, that is when the

source points coincide with the observation points the value of the generic integral (19) and (20) is zero (Gibson (2007)).

$$\hat{n}(\overline{\rho}) \times \int_{\delta S} \overline{K}\overline{\rho}' \times \nabla' G(\overline{\rho},\overline{\rho}')\, d\overline{\rho}'\Big|_{s^+} = \overline{K}(\overline{\rho})/2. \qquad (21)$$

For triangle/pulse and sinusoid/pulse method, the basis function is differentiable and the pulse testing function absorbs the derivative in the generic integral (18) by using the method of finite difference (Peterson (1998)), that is

$$\int f_m(\overline{\rho})\hat{t}(\overline{\rho}) \cdot \nabla\nabla \cdot \overline{X}(K\hat{t})\, d\overline{\rho} = [\nabla \cdot \overline{X}(K\hat{t})]_{\rho_1}^{\rho_2}. \qquad (22)$$

For triangle/ triangle, triangle/ sinusoid, sinusoid/ triangle and sinusoid/ sinusoid method, the generic integral (18) is evaluated by distributing the del operator (Gibson (2007)), that is given as

$$\int f_m(\overline{\rho})\hat{t}(\overline{\rho}) \cdot \nabla\nabla \cdot \overline{X}(K\hat{t})\, d\overline{\rho} = -\int \nabla \cdot [f_m(\overline{\rho})\hat{t}(\overline{\rho})]\nabla \cdot \overline{X}(K\hat{t})\, d\overline{\rho}. \qquad (23)$$

The singular integrals are evaluated through the use of inner analytical integration and outer numerical integration. Details of numerical implementation can be found in (Gibson (2007)). The small argument approximation for the Hankel function is utilised when dealing with singular integrals.

$$H_0^{(2)}(k\,|\,\overline{\rho} - \overline{\rho}'|) \cong 1 - j\frac{2}{\pi}\ln(\frac{\gamma k\,|\,\overline{\rho} - \overline{\rho}'|}{2}) \qquad (24)$$

The value of γ in equation (24) is equal to 1.781072418. The inner analytical integration is given in the Appendix.

3. METHODOLOGY

For the Gauss quadrature computing technique, the technique of computing is as follows. For the TT, TS, ST and SS method, the generic integrals are evaluated at 6 quadrature points for the inner and outer numerical integration over the segment length h. From Figure 1(a) and 1(b), $t_{m+1} - t_m = t_m - t_{m+1} = h$ for triangle and sinusoid testing function whereas $t_{m+1/2} - t_m = t_m - t_{m-1/2} = h/2$ for pulse testing function. For TP and

252

SP method, due to the fact that the pulse spans from the half length of a particular segment length to the half length of the adjacent segment length whereas the triangle function or the sinusoid function spans over 2 adjacent segment length, the numerical integration for singular and non-singular generic integrals is performed by decomposing the integrals of a particular basis function into 4 segments of the same length, and each segment is evaluated over 3 quadrature points for the inner and outer numerical integration. The pulse tested is decomposed into 2 segments, and each segment is evaluated over 3 quadrature points. For that, we have maintained the same number of quadrature points for the inner and outer numerical integrations for every segment length h. The value of the wavenumber in the sinusoid basis and testing function is taken to be equal to the freespace wavenumber.
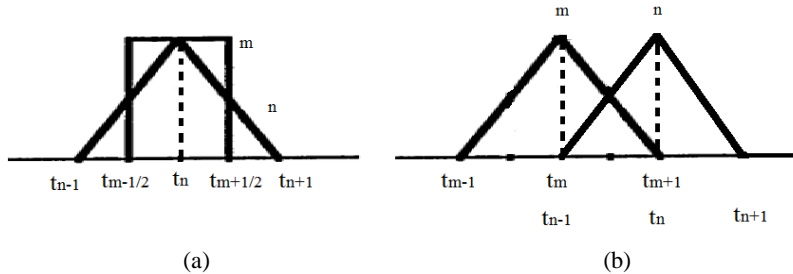

Figure 1: (a) Triangle basis function and pulse testing function (b) Triangle basis function and triangle testing function where the *m-th* testing function overlaps with the *n-th* triangle basis function

For the staircase approximation computing technique, the technique of computing is as follows. For the TT, TS, ST and SS method; the generic integrals are evaluated by using a representation of 6 pulses/intervals for the inner and outer numerical integration over the segment length h where this is similar to the number of quadrature points as in the evaluation for sinusoid and triangle function using the Gauss quadrature technique. As noted previously, for TP and SP method, due to the fact that the pulse spans from the half length of a particular segment length to the half length of the adjacent segment length whereas the triangle and sinusoid basis function spans over 2 adjacent segment length, the numerical integration for singular and non-singular generic integrals is performed by decomposing the integrals of a particular basis function into 4 segments of the same length, and each segment is evaluated by using a representation of 3 pulses/intervals for the inner and outer numerical integration. The pulse tested is decomposed into 2 segments, and each segment is evaluated by using a representation of 3 pulses/intervals.

The number of pulses/intervals used for the pulse testing function in the staircase approximation technique is similar to the number of quadrature points used for the pulse testing function evaluated using Gauss quadrature technique. For that, we have maintained the same number of pulses/intervals for the inner and outer numerical integrations for every segment length h. For illustration purposes, Figure 2 shows the representation of the pulse function, triangle function and sinusoid function using 6 pulses/intervals over the segment length h where $h = t_2 - t_1$ for Figure 2(a), whereas for Figure 2(b) and Figure 2(c), $h = t_2 - t_1 = t_3 - t_2$.
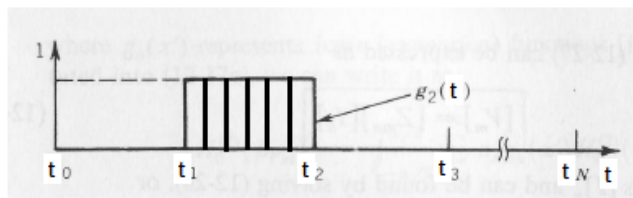
(a)
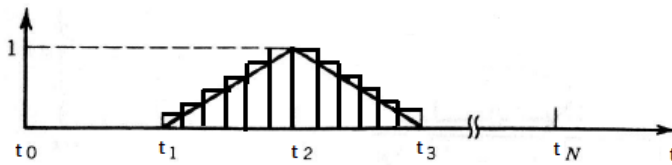
(b)
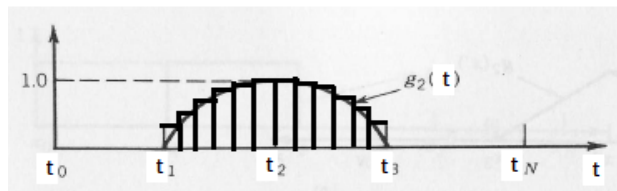
(c)

Figure 2: Staircase approximation of (a) pulse (b) triangle (c) sinusoid function using 6 pulses/intervals over segment length h.

In both computing techniques, the flat-faceted mesh employed in our codes is regular with the segment length h. The mesh element width is $h = \lambda / n$ where λ is the wave length of the incident plane wave and n is the number of samples/wavelength (Davis *et al.* (2005)). Comparison is made for identical solution conditions, such as the number of expansion functions, the numerical integration of Green's function and similar mesh density. The relative error is given by

254

$$\delta x = \frac{\Delta x}{x} = \frac{|x_0 - x|}{x} \qquad (25)$$

where x is true value of a quantity and x_0 is the calculated values. The mean relative error of the surface current density is computed for both computing techniques at different number of samples/wavelength.

4. VALIDATION AND VERIFICATION

The TE scattering from a hollow dielectric cylinder with $b = (0.0819*2/\pi)$ meter and $a = (0.0819*2*0.6/\pi)$ where b is the outer radius and a is the inner radius with the relative permittivity, $\varepsilon_r = 4$ and relative permeability $\mu_r = 1$ at 915 MHz is considered. The incident magnetic plane wave of unity magnitude. Due to inadequate space in the paper only 3 angles are shown for brevity. Good agreement is observed with the exact eigenfunction series solution (Bussey *et al.* (1975)) regardless of the basis and testing function used on the different surface integral equations.

TABLE 1: Magnitude of the magnetic current density (unit: V/m) on the outer layer of a hollow dielectric cylinder using Gauss quadrature technique

Method	Angle(deg.)	EFIE	MFIE	PMCHW	Muller	Exact
SP	0	328.083	327.3831	328.1792	328.3338	328.1137
	90	200.0225	199.2938	200.45	200.1301	200.0712
	180	333.2926	332.9305	334.1597	333.3484	333.4593
SS	0	328.0691	327.611	328.0877	328.3244	328.1137
	90	199.9407	199.5369	200.2318	200.0557	200.0712
	180	333.3099	333.0443	333.7805	333.3951	333.4593
ST	0	328.0689	327.6109	328.0879	328.3229	328.1137
	90	199.9408	199.5368	200.2321	200.055	200.0712
	180	333.31	333.0443	333.7806	333.3945	333.4593
TP	0	328.1909	327.4925	328.2859	328.4419	328.1137
	90	200.0883	199.3611	200.5151	200.196	200.0712
	180	333.4022	333.0409	334.2682	333.458	333.4593
TS	0	328.2065	327.7206	328.0815	328.6916	328.1137
	90	200.0665	199.6044	200.202	200.4312	200.0712
	180	333.4816	333.1548	333.7958	333.8129	333.4593
TT	0	328.1768	327.7205	328.1948	328.4309	328.1137
	90	200.0066	199.6043	200.2969	200.1208	200.0712
	180	333.4197	333.1548	333.8887	333.5042	333.4593

TABLE 2: Magnitude of the magnetic current density (unit : V/m) on the outer layer of a hollow dielectric cylinder using staircase approximation technique

Method	Angle(deg.)	EFIE	MFIE	PMCHW	Muller	Exact
SP	0	328.0967	326.8061	327.7181	327.8137	328.1137
	90	199.6694	198.2682	199.5291	200.0121	200.0712
	180	333.0646	332.7043	334.2627	333.3858	333.4593
SS	0	328.1605	326.807	327.8527	327.8834	328.1137
	90	199.6267	198.2673	199.4844	199.9548	200.0712
	180	333.1116	332.7054	334.1524	333.4443	333.4593
ST	0	328.1607	326.8069	327.8523	327.8831	328.1137
	90	199.6267	198.2671	199.4853	199.954	200.0712
	180	333.1115	332.7053	334.1538	333.4434	333.4593
TP	0	328.2065	326.9164	327.8258	327.9239	328.1137
	90	199.7359	198.3356	199.5953	200.0786	200.0712
	180	333.1753	332.8159	334.3742	333.4965	333.4593
TS	0	328.2706	326.9173	327.9612	327.9936	328.1137
	90	199.6937	198.3347	199.5516	200.0213	200.0712
	180	333.223	332.817	334.2645	333.5551	333.4593
TT	0	328.2705	326.9171	327.9601	327.9933	328.1137
	90	199.6932	198.3345	199.5514	200.0204	200.0712
	180	333.2223	332.8169	334.2652	333.5541	333.4593

5. RESULTS AND DISCUSSION

The TE scattering by a hollow dielectric cylinder with $b = (0.0819*2/\pi)$ meter and $a = (0.0819*2*0.6/\pi)$ where b is the outer radius and a is the inner radius at the frequency of 915 MHz is considered. For the inner layer, $\varepsilon_r = 1$ and $\mu_r = 1$ whilst for the outer layer, $\mu_r = 1$ and different values of ε_r are selected. Numerical data in terms of variation of outer layer surface magnetic current density mean relative error with samples/wavelength for $\varepsilon_r = 77.3-j37.2$ (Ikediala *et al.* (2002)), $\varepsilon_r = 31.7-j136.8$ (Yifen *et al.* (2003)), and $\varepsilon_r = 75-j300$ (Peterson (1994)) is tabulated in from Table 3 to Table 8 for both computing techniques at the frequency of 915 MHz. The variation of mean relative error with samples/wavelength is tabulated in Table 3, 4 and 5 using the Gauss quadrature technique. The number of samples/wavelength, n used is 30, 40, 50, 60 and 70 samples/λ_0 for the outer radius and inner radius where λ_0 is the free space wavelength. This corresponds to the MoM impedance matrix size of 96 by 96, 128 by 128, 160 by 160, 192 by 192 and 224 by 224 by taking the overall surface electric and magnetic current density into account. The computer storage requirements is denoted by the size of the matrix because the larger the matrix, the computer storage requirement needed will be higher and the computing time will also increase.

The location where the testing function overlaps the basis function
is the location where the source and observation points coincide and the
integrals involved in the integration process would be singular. The
analytical evaluation of the singular integrals using small argument
approximation of the Hankel function as in (Gibson (2007)) would require
that the length of the intervals involved in the inner analytical integration of
the Hankel function to be as short as possible because the smaller the value
of the Hankel function argument, the evaluation of the singular integrals
would be much more accurate. From equation (8), (9), and (24), the value
of f, μ, ε and $|\bar{\rho} - \bar{\rho}'|$, will determine on how small the value of the
argument $k|\bar{\rho} - \bar{\rho}'|$ will be for the Hankel function and this will determine
the error contamination and therefore the accuracy in the numerical
evaluation of singular integrals. The possible maximum value of $|\bar{\rho} - \bar{\rho}'|$ in
the inner analytical integration of overlapping basis and testing function due
to different testing point locations of the outer numerical integration for the
pulse testing function is slightly less than $h/2$ whilst for the triangle and
sinusoid testing function is slightly less than h. This is because the width of
overlapping basis and testing function for TT, TS, SS and ST is higher than
the TP and SP method.

TABLE 3: Mean relative error for hollow dielectric cylinder with $\varepsilon_r = 77.3 - j37.2$ using
Gauss quadrature

n	Equation	SP	SS	ST	TP	TS	TT
30	EFIE	0.0109	0.1023	0.1023	0.0137	0.1063	0.1062
	MFIE	0.0372	0.1519	0.1520	0.0341	0.1493	0.1494
	PMCHW	0.0394	0.1608	0.1609	0.0367	0.1583	0.1584
	Muller	0.0606	0.6030	0.6032	0.0643	0.6049	0.6087
40	EFIE	0.0052	0.0502	0.0502	0.0066	0.0523	0.0523
	MFIE	0.0184	0.0820	0.0820	0.0166	0.0803	0.0803
	PMCHW	0.0196	0.0872	0.0872	0.0182	0.0856	0.0856
	Muller	0.0270	0.2402	0.2403	0.0291	0.2414	0.2427
50	EFIE	0.0033	0.0284	0.0283	0.0038	0.0297	0.0296
	MFIE	0.0104	0.0488	0.0488	0.0093	0.0477	0.0477
	PMCHW	0.0113	0.0520	0.0520	0.0104	0.0509	0.0509
	Muller	0.0144	0.1260	0.1260	0.0157	0.1268	0.1274
60	EFIE	0.0024	0.0176	0.0176	0.0025	0.0185	0.0185
	MFIE	0.0064	0.0314	0.0314	0.0057	0.0306	0.0306
	PMCHW	0.0071	0.0334	0.0334	0.0066	0.0326	0.0326
	Muller	0.0086	0.0758	0.0758	0.0095	0.0763	0.0767
70	EFIE	0.0018	0.0117	0.0117	0.0018	0.0124	0.0124
	MFIE	0.0042	0.0213	0.0213	0.0037	0.0207	0.0207
	PMCHW	0.0048	0.0227	0.0227	0.0044	0.0222	0.0222
	Muller	0.0055	0.0496	0.0496	0.0062	0.0500	0.0503

TABLE 4: Mean relative error for hollow dielectric cylinder with $\varepsilon_r = 31.7 - j136.8$ using Gauss quadrature

n	Equation	SP	SS	ST	TP	TS	TT
30	EFIE	0.041	0.2169	0.2169	0.0429	0.2191	0.219
	MFIE	0.0391	0.1988	0.1988	0.0377	0.1978	0.1979
	PMCHW	0.0399	0.2013	0.2014	0.0388	0.2004	0.2005
	Muller	0.0988	0.4852	0.4852	0.1004	0.4867	0.4868
40	EFIE	0.0203	0.1129	0.1129	0.0214	0.114	0.114
	MFIE	0.0185	0.1064	0.1064	0.0177	0.1056	0.1057
	PMCHW	0.019	0.1078	0.1078	0.0183	0.1071	0.1071
	Muller	0.0484	0.2641	0.2642	0.0494	0.265	0.2651
50	EFIE	0.0117	0.0666	0.0666	0.0125	0.0673	0.0673
	MFIE	0.01	0.0634	0.0634	0.0095	0.0628	0.0628
	PMCHW	0.0104	0.0642	0.0642	0.01	0.0637	0.0637
	Muller	0.0277	0.1555	0.1555	0.0284	0.1561	0.1561
60	EFIE	0.0075	0.0428	0.0428	0.008	0.0433	0.0433
	MFIE	0.006	0.0408	0.0408	0.0056	0.0404	0.0404
	PMCHW	0.0062	0.0414	0.0414	0.006	0.041	0.041
	Muller	0.0175	0.0992	0.0992	0.018	0.0997	0.0997
70	EFIE	0.0051	0.0293	0.0293	0.0055	0.0297	0.0297
	MFIE	0.0038	0.0278	0.0278	0.0036	0.0275	0.0275
	PMCHW	0.004	0.0282	0.0282	0.0039	0.0279	0.0279
	Muller	0.0119	0.0674	0.0674	0.0123	0.0678	0.0678

TABLE 5: Mean relative error for hollow dielectric cylinder with $\varepsilon_r = 75 - j300$ using Gauss quadrature

n	Equation	SP	SS	ST	TP	TS	TT
30	EFIE	0.11	0.515	0.5151	0.112	0.5181	0.5181
	MFIE	0.1031	0.4189	0.419	0.1017	0.4183	0.4184
	PMCHW	0.1038	0.4208	0.4209	0.1025	0.4202	0.4204
	Muller	0.2663	0.8673	0.8674	0.2678	0.8688	0.8689
40	EFIE	0.0555	0.2806	0.2806	0.0566	0.2819	0.2819
	MFIE	0.0522	0.2484	0.2485	0.0513	0.2479	0.2479
	PMCHW	0.0526	0.2497	0.2498	0.0517	0.2492	0.2493
	Muller	0.1337	0.6048	0.6048	0.1346	0.6056	0.6057
50	EFIE	0.0322	0.1704	0.1704	0.033	0.1712	0.1712
	MFIE	0.0299	0.1567	0.1567	0.0293	0.1562	0.1562
	PMCHW	0.0301	0.1575	0.1576	0.0295	0.1571	0.1571
	Muller	0.0769	0.3996	0.3997	0.0775	0.4002	0.4003
60	EFIE	0.0205	0.1117	0.1117	0.0211	0.1122	0.1122
	MFIE	0.0187	0.1048	0.1048	0.0182	0.1044	0.1044
	PMCHW	0.0188	0.1053	0.1053	0.0184	0.105	0.105
	Muller	0.0486	0.2666	0.2666	0.0491	0.267	0.2671
70	EFIE	0.014	0.0774	0.0774	0.0144	0.0778	0.0778
	MFIE	0.0124	0.0735	0.0735	0.0121	0.0731	0.0731
	PMCHW	0.0125	0.0738	0.0739	0.0122	0.0735	0.0736
	Muller	0.0329	0.1848	0.1848	0.0333	0.1851	0.1851

TABLE 6: Mean relative error for hollow dielectric cylinder with $\varepsilon_r = 77.3 - j37.2$ using staircase approximation

n	Equation	SP	SS	ST	TP	TS	TT
30	EFIE	0.0313	0.0316	0.0315	0.0297	0.0305	0.0304
	MFIE	0.0355	0.0356	0.0356	0.0378	0.0379	0.0379
	PMCHW	0.0425	0.0405	0.0406	0.0449	0.0429	0.0430
	Muller	0.0953	0.0960	0.0960	0.0931	0.0938	0.0938
40	EFIE	0.0218	0.0224	0.0223	0.0209	0.0219	0.0218
	MFIE	0.0285	0.0286	0.0286	0.0299	0.0299	0.0299
	PMCHW	0.0336	0.0322	0.0322	0.0350	0.0336	0.0336
	Muller	0.0714	0.0716	0.0716	0.0702	0.0704	0.0704
50	EFIE	0.0167	0.0173	0.0173	0.0162	0.0170	0.0170
	MFIE	0.0238	0.0238	0.0238	0.0247	0.0247	0.0247
	PMCHW	0.0277	0.0266	0.0267	0.0286	0.0275	0.0276
	Muller	0.0570	0.0570	0.0570	0.0562	0.0562	0.0562
60	EFIE	0.0135	0.0141	0.0141	0.0132	0.0139	0.0139
	MFIE	0.0204	0.0204	0.0204	0.0210	0.0210	0.0210
	PMCHW	0.0236	0.0227	0.0227	0.0242	0.0234	0.0234
	Muller	0.0474	0.0473	0.0473	0.0469	0.0468	0.0468
70	EFIE	0.0113	0.0119	0.0119	0.0111	0.0118	0.0118
	MFIE	0.0178	0.0178	0.0178	0.0183	0.0183	0.0183
	PMCHW	0.0205	0.0198	0.0198	0.0210	0.0203	0.0203
	Muller	0.0406	0.0405	0.0405	0.0402	0.0401	0.0401

TABLE 7: Mean relative error for hollow dielectric cylinder with $\varepsilon_r = 31.7 - j136.8$ using staircase approximation

n	Equation	SP	SS	ST	TP	TS	TT
30	EFIE	0.0429	0.0413	0.0413	0.0406	0.0394	0.0393
	MFIE	0.0494	0.0494	0.0494	0.0524	0.0525	0.0525
	PMCHW	0.0535	0.0517	0.0517	0.0566	0.0548	0.0548
	Muller	0.092	0.0896	0.0896	0.0897	0.0874	0.0874
40	EFIE	0.0321	0.0309	0.0308	0.0308	0.0297	0.0297
	MFIE	0.0369	0.037	0.037	0.0386	0.0387	0.0387
	PMCHW	0.0399	0.0386	0.0387	0.0416	0.0404	0.0404
	Muller	0.07	0.0681	0.0681	0.0687	0.0668	0.0668
50	EFIE	0.0256	0.0246	0.0246	0.0247	0.0238	0.0238
	MFIE	0.0295	0.0295	0.0295	0.0306	0.0306	0.0306
	PMCHW	0.0318	0.0309	0.0309	0.0329	0.032	0.032
	Muller	0.0565	0.0549	0.0549	0.0556	0.054	0.054
60	EFIE	0.0213	0.0204	0.0204	0.0207	0.0199	0.0199
	MFIE	0.0246	0.0246	0.0246	0.0253	0.0253	0.0253
	PMCHW	0.0264	0.0257	0.0257	0.0272	0.0264	0.0265
	Muller	0.0473	0.0459	0.0459	0.0467	0.0453	0.0453
70	EFIE	0.0182	0.0175	0.0175	0.0178	0.0171	0.0171
	MFIE	0.021	0.0211	0.0211	0.0216	0.0216	0.0216
	PMCHW	0.0226	0.022	0.022	0.0232	0.0226	0.0226
	Muller	0.0407	0.0395	0.0395	0.0403	0.0391	0.0391

TABLE 8: Mean relative error for hollow dielectric cylinder with $\varepsilon_r = 75 - j300$ using staircase approximation

n	Equation	SP	SS	ST	TP	TS	TT
30	**EFIE**	0.0632	0.0624	0.0623	0.0611	0.0605	0.0604
	MFIE	0.0718	0.0718	0.0718	0.0746	0.0747	0.0747
	PMCHW	0.0755	0.0737	0.0737	0.0784	0.0766	0.0767
	Muller	0.1347	0.1332	0.1331	0.1325	0.131	0.131
40	**EFIE**	0.0475	0.0468	0.0468	0.0463	0.0457	0.0457
	MFIE	0.0535	0.0536	0.0535	0.0551	0.0552	0.0551
	PMCHW	0.0562	0.055	0.055	0.0578	0.0566	0.0566
	Muller	0.1035	0.1022	0.1022	0.1022	0.101	0.101
50	**EFIE**	0.038	0.0374	0.0374	0.0372	0.0367	0.0366
	MFIE	0.0427	0.0427	0.0427	0.0437	0.0437	0.0437
	PMCHW	0.0447	0.0438	0.0438	0.0457	0.0448	0.0449
	Muller	0.0839	0.0829	0.0829	0.0831	0.082	0.082
60	**EFIE**	0.0316	0.0311	0.0311	0.0311	0.0306	0.0306
	MFIE	0.0355	0.0355	0.0355	0.0362	0.0362	0.0362
	PMCHW	0.0371	0.0364	0.0364	0.0378	0.0371	0.0371
	Muller	0.0706	0.0697	0.0697	0.07	0.0691	0.0691
70	**EFIE**	0.0271	0.0266	0.0266	0.0267	0.0263	0.0262
	MFIE	0.0304	0.0304	0.0304	0.0309	0.0309	0.0309
	PMCHW	0.0317	0.0311	0.0312	0.0323	0.0317	0.0317
	Muller	0.0609	0.0601	0.0601	0.0604	0.0596	0.0596

Using smaller impedance matrix, the evaluation in the singular integrals would give the least error contamination when SP and TP method is used compared to the SS, ST, TS and TT method due to larger intervals of the inner analytical integration of the Hankel function when dealing with singular integrals. The error due to the small argument approximation is being amplified by the value of high permittivity which is used in the calculation of the wave number in the Hankel function. Therefore faster convergence is achieved when the SP method is used compared to the SS and ST method. Similarly, faster convergence is achieved when the TP method is used compared to the TS and TT method.

The error contamination is much more pronounce in the Muller integral equation than any other integral equation when the SS, ST, TS and TT method is used compared to the SP and TP method because the value of relative permittivity is more abundant in the Muller integral equation than any other integral equation and this intensifies the error due to the small argument approximation when a high relative permittivity is used. Therefore, when dealing with high permittivity object, a smaller impedance matrix size that give less error contamination can be achieved with the SP and TP method than the SS, ST, TS and TT method under the Gauss quadrature technique.

The variation of outer layer surface magnetic current density mean relative error with samples/wavelength using staircase approximation technique is tabulated in Table 6, 7 and 8 by applying the same parameter value as in the Gauss quadrature technique at the frequency of 915 MHz. For the staircase approximation technique, the basis and testing function are approximated by intervals/pulses. The evaluation of singular integrals using the staircase approximation technique utilises the small argument approximation of the Hankel function for overlapping intervals/pulses of basis and testing function (Ayyildiz (2006)). The small argument approximation of the Hankel function is not used when the intervals/pulses do not overlap even though the basis and testing function overlaps. The length of the interval for the inner analytical integration of the Hankel function for overlapping basis and testing intervals/pulses is maintained to be the same for all the different basis and testing function. Therefore, the effect of high permittivity does not greatly affect the difference in the convergence due to different basis and testing function.

In both computing techniques, we have utilised the small argument approximation of the Hankel function in the evaluation of singular integrals. For singular and non-singular integrals, the same number of computation points is used for both computing techniques (which is the quadrature points for the Gauss quadrature technique and intervals/pulses for the staircase approximation technique). The error contamination due to the small argument approximation of the Hankel function is not negligible when a smaller impedance matrix size is required for high permittivity scatterers. Although the error of numerical solution due to the staircase approximation technique deteriorates when a smaller impedance matrix size is required for high permittivity object, the difference in the error contamination due to different basis and testing function is not as distinguishable as in the Gauss quadrature technique.

For high permittivity object, it takes higher samples/wavelength for the error due to Gauss quadrature to be less than the error due to staircase approximation when the SS, ST, TS and TT method is used compared to the SP and TP method. This implies that a larger matrix size is required by the SS, ST, TS and TT method than the SP and TP method for the Gauss quadrature to be more accurate than the staircase approximation. As a result, for high permittivity objects, the memory requirements needed for the Gauss quadrature error to be less than the staircase approximation error would be higher when the SS, ST, TS and TT method is used compared to the SP and TP method.

This indicate that different basis and testing function affect the efficiency of different numerical implementations in terms of matrix size when dealing with high permittivity objects. From the numerical experimentation, it can be deduced that when a smaller impedance matrix size is desired for large size high permittivity object, the SS, ST, TS and TT method give higher amount of error contamination for a higher number of integral equations compared to the SP and TP method when the Gauss quadrature technique is used. On the other hand, it can be deduced that the error contamination due to different testing function is almost similar for a higher number of integral equations using the staircase approximation technique when a smaller impedance matrix size is required for large size high permittivity object.

The TE scattering by a dielectric coated impedance cylinder with $kb = 4$ and $ka = 3$ (Kishk (1991)) at the frequency of 300 MHz is considered. For the outer layer, $\varepsilon_r = 4$ and $\mu_r = 1$. Different sets of value are selected for the inner core. Numerical data for $\varepsilon_r = 8$-j16 and $\mu_r = 2$-j4 (Kishk (1991)) is tabulated in Table 9. Numerical data for $\varepsilon_r = 12$-j24 and $\mu_r = 3$-j6 is tabulated in Table 10. Numerical data for $\varepsilon_r = 16$-j32 and $\mu_r = 4$-j8 is tabulated in Table 11. For the different sets of ε_r and μ_r used, $\eta_1 = 0.25$ where it is used in the impedance boundary condition (IBC) and numerical data is tabulated in Table 12. The IBC is used to simplify the scattering problem when the relative permittivity scatterer is large (Peterson, 1998). In order for the IBC to be valid, the fields must decay within the IBC region which must be sufficiently lossy where the absorption and attenuation of waves is influenced by the loss factor (Peterson, 1998).

The variation of outer layer magnetic current density mean relative error with samples per wavelength is tabulated in Table 9, 10, 11 and 12. The samples/wavelength, n used is 30, 40, 50, 60 and 70 samples/ λ_0 where λ_0 is the free space wavelength. This corresponds to the MoM impedance matrix size of 420 by 420, 560 by 560, 700 by 700, 840 by 840 and 980 by 980 under the exact boundary condition (EBC) whilst under the impedance boundary condition (IBC) this corresponds to the impedance matrix size of 330 by 330, 440 by 440, 550 by 550, 660 by 660 and 770 by 770 by taking the overall surface electric and magnetic current into account. Similar samples/wavelength is applied on the outer radius and inner radius of the dielectric coated impedance cylinder. The same subroutine has been used in the calculation of the generic integrals under the exact and impedance boundary conditions.

TABLE 9: Mean relative error for dielectric coated impedance cylinder with
$\varepsilon_r = 8 - j16$ and $\mu_r = 2 - j4$ using Gauss quadrature and EBC

n	Equation	SP	SS	ST	TP	TS	TT
30	EFIE	0.018	0.0955	0.0956	0.0212	0.0983	0.099
	MFIE	0.0191	0.092	0.0921	0.0165	0.0894	0.0894
	PMCHW	0.0034	0.0083	0.0083	0.0054	0.0102	0.0104
	Muller	0.1532	0.6713	0.6715	0.1545	0.6747	0.6749
40	EFIE	0.0091	0.0474	0.0474	0.0108	0.0488	0.0492
	MFIE	0.0098	0.047	0.047	0.0084	0.0454	0.0454
	PMCHW	0.0027	0.0024	0.0024	0.0037	0.0036	0.0038
	Muller	0.0771	0.3741	0.3742	0.0777	0.3755	0.3756
50	EFIE	0.0057	0.0273	0.0273	0.0067	0.0282	0.0284
	MFIE	0.006	0.0275	0.0275	0.0052	0.0265	0.0265
	PMCHW	0.0024	0.0019	0.0019	0.003	0.0026	0.0026
	Muller	0.0449	0.2276	0.2277	0.0453	0.2284	0.2284
60	EFIE	0.0041	0.0173	0.0174	0.0048	0.0179	0.0181
	MFIE	0.0043	0.0177	0.0177	0.0037	0.017	0.017
	PMCHW	0.0023	0.002	0.002	0.0027	0.0025	0.0024
	Muller	0.0289	0.1486	0.1486	0.0292	0.149	0.149
70	EFIE	0.0033	0.0118	0.0118	0.0038	0.0122	0.0124
	MFIE	0.0034	0.0122	0.0122	0.003	0.0117	0.0117
	PMCHW	0.0023	0.0021	0.0021	0.0025	0.0024	0.0024
	Muller	0.0201	0.1025	0.1025	0.0203	0.1028	0.1028

TABLE 10: Mean relative error for dielectric coated impedance cylinder with
$\varepsilon_r = 12 - j24$ and $\mu_r = 3 - j6$ using Gauss quadrature and EBC

n	Equation	SP	SS	ST	TP	TS	TT
30	EFIE	0.048	0.2558	0.256	0.0512	0.2591	0.2599
	MFIE	0.0485	0.2301	0.2302	0.0457	0.228	0.2281
	PMCHW	0.0046	0.0607	0.0607	0.0069	0.0627	0.063
	Muller	0.5226	1.6528	1.6531	0.5251	1.6596	1.6598
40	EFIE	0.0236	0.1272	0.1272	0.0254	0.1288	0.1292
	MFIE	0.0245	0.1208	0.1208	0.0229	0.1194	0.1194
	PMCHW	0.0027	0.0159	0.0159	0.0039	0.0171	0.0172
	Muller	0.2815	1.0906	1.0908	0.2825	1.0934	1.0935
50	EFIE	0.0137	0.0739	0.0739	0.0148	0.0749	0.0751
	MFIE	0.0144	0.0721	0.0721	0.0134	0.0711	0.0711
	PMCHW	0.0024	0.006	0.006	0.0031	0.0067	0.0068
	Muller	0.1684	0.7376	0.7377	0.1689	0.7389	0.739
60	EFIE	0.0088	0.0473	0.0473	0.0096	0.0479	0.0481
	MFIE	0.0094	0.0468	0.0468	0.0087	0.0461	0.0461
	PMCHW	0.0023	0.0031	0.0031	0.0027	0.0036	0.0036
	Muller	0.1091	0.5151	0.5151	0.1094	0.5158	0.5158
70	EFIE	0.0062	0.0323	0.0323	0.0068	0.0328	0.0329
	MFIE	0.0067	0.0324	0.0324	0.0062	0.0318	0.0318
	PMCHW	0.0023	0.0022	0.0022	0.0025	0.0025	0.0026
	Muller	0.0752	0.3715	0.3715	0.0754	0.3719	0.3719

TABLE 11: Mean relative error for dielectric coated impedance cylinder with
$\varepsilon_r = 16 - j32$ and $\mu_r = 4 - j8$ using Gauss quadrature and EBC

n	Equation	SP	SS	ST	TP	TS	TT
30	EFIE	0.0968	0.5234	0.5238	0.1002	0.5276	0.5285
	MFIE	0.0942	0.4294	0.4296	0.0915	0.4281	0.4283
	PMCHW	0.0111	0.24	0.2402	0.0134	0.2425	0.2429
	Muller	1.0955	2.5076	2.5079	1.1	2.5177	2.5177
40	EFIE	0.0479	0.257	0.2571	0.0497	0.2588	0.2593
	MFIE	0.048	0.2311	0.2312	0.0464	0.2299	0.23
	PMCHW	0.004	0.0627	0.0627	0.0053	0.0638	0.0639
	Muller	0.6528	1.9083	1.9086	0.6545	1.9127	1.9129
50	EFIE	0.0277	0.1491	0.1491	0.0288	0.1501	0.1504
	MFIE	0.0282	0.1402	0.1403	0.0272	0.1393	0.1394
	PMCHW	0.0026	0.0223	0.0223	0.0033	0.023	0.023
	Muller	0.4128	1.4364	1.4366	0.4136	1.4386	1.4387
60	EFIE	0.0176	0.0957	0.0957	0.0184	0.0964	0.0965
	MFIE	0.0182	0.0922	0.0922	0.0175	0.0916	0.0916
	PMCHW	0.0023	0.0098	0.0098	0.0027	0.0103	0.0103
	Muller	0.2759	1.0862	1.0863	0.2764	1.0874	1.0875
70	EFIE	0.0121	0.0657	0.0657	0.0126	0.0662	0.0663
	MFIE	0.0126	0.0643	0.0643	0.0121	0.0638	0.0638
	PMCHW	0.0023	0.0052	0.0052	0.0025	0.0056	0.0056
	Muller	0.1934	0.831	0.8311	0.1937	0.8317	0.8318

TABLE 12: Mean relative error for dielectric coated impedance cylinder using Gauss
quadrature and IBC

n	Equation	SP	SS	ST	TP	TS	TT
30	EFIE	0.0118	0.0109	0.0109	0.0093	0.0094	0.0094
	MFIE	0.0113	0.0115	0.0115	0.0087	0.0092	0.0092
	PMCHW	0.0112	0.0114	0.0115	0.0086	0.0089	0.0089
	Muller	0.0108	0.0099	0.0099	0.0082	0.0087	0.0088
40	EFIE	0.0117	0.0104	0.0104	0.0103	0.0092	0.0092
	MFIE	0.0114	0.0111	0.0111	0.01	0.0096	0.0096
	PMCHW	0.0113	0.0113	0.0113	0.0099	0.0098	0.0098
	Muller	0.0112	0.0102	0.0102	0.0097	0.009	0.0089
50	EFIE	0.0117	0.0109	0.0109	0.0108	0.0101	0.01
	MFIE	0.0115	0.0113	0.0113	0.0106	0.0103	0.0103
	PMCHW	0.0115	0.0114	0.0114	0.0105	0.0105	0.0104
	Muller	0.0114	0.0108	0.0108	0.0104	0.01	0.0099
60	EFIE	0.0117	0.0112	0.0112	0.0111	0.0106	0.0105
	MFIE	0.0116	0.0114	0.0114	0.0109	0.0107	0.0107
	PMCHW	0.0115	0.0115	0.0115	0.0109	0.0108	0.0108
	Muller	0.0115	0.0112	0.0112	0.0108	0.0106	0.0105
70	EFIE	0.0117	0.0113	0.0113	0.0113	0.0109	0.0109
	MFIE	0.0116	0.0115	0.0115	0.0111	0.011	0.011
	PMCHW	0.0116	0.0116	0.0116	0.0111	0.0111	0.0111
	Muller	0.0115	0.0114	0.0114	0.0111	0.0109	0.0109

Under the exact boundary condition (EBC), the EBC is applied on the outer layer and the core of the dielectric coated impedance cylinder whilst under the impedance boundary condition (IBC), the IBC is applied only on the inner core and the EBC is applied on the outer layer of the dielectric coated impedance cylinder (Kishk (1991)). Therefore, the governing integral equations using the EBC and IBC are only different at the core of the dielectric coated impedance cylinder.

When the EBC is utilised for the dielectric coated impedance cylinder, the relative permittivity and permeability of the core is used in the calculation of the wave number of the Hankel function and as a result, the SP and TP method give faster convergence than the SS, ST, TS and TT method. Under the EBC, the difference in the convergence due to different basis and testing function for the PMCHW integral equation is not as distinguishable as the EFIE and MFIE. This is may be attributed from the equation governing the interior and exterior region is separated in the EFIE and MFIE whereas it is coupled in the PMCHW integral equation.

Another factor this is that for the PMCHW integral equation, only 2 governing equations on the core of the dielectric coated impedance cylinder under the EBC is affected by the error due the small argument approximation of Hankel function instead of 4 governing equations on the core and outer layer as in the case of the high permittivity hollow dielectric cylinder considered previously in Table 3, 4, and 5 since the location of high permittivity is in the core and not on the outer layer of the dielectric coated impedance cylinder.

Though the equation governing the interior and exterior region is coupled in the Muller integral equation, the value of the relative permittivity and permeability is abundant in the integral equation that intensifies the error due to the small argument approximation of the Hankel function. Therefore, the difference in the convergence due to different basis and testing function for the Muller integral equation is more distinguishable compared to the PMCHW integral equation when the EBC is used.

When the IBC is utilised, the relative permittivity and permeability of the core is not used in the calculation of the wave number of the Hankel function and it is only used for the calculation of the surface impedance, which is given by equation (15). Therefore, the error due to the small argument approximation of Hankel function is much more pronounced when the EBC is used compared to the IBC. As a result, the difference in

the convergence due to different basis and testing function under the IBC is not as distinguishable as under the EBC. This is clearly seen for the Muller integral equation compared to any other integral equation because the error due to the small argument approximation of the Hankel function is intensified by the abundant relative permittivity and permeability when the EBC is used whilst under the IBC, the difference in the convergence due to different basis and testing function for the Muller integral equation is almost indistinguishable.

The convergence due to different basis and testing function under the IBC for highly lossy object is not as distinguishable as under the EBC for a higher number of integral equations even though the SS, ST, TS and TP method converge slower than the SP and TP method for a higher number of integral equations under the EBC. This indicate that any of the basis and testing functions can be selected under the IBC although the SP and TP method converge faster than the SS, ST, TS and TT method under the EBC. The SS, ST, TS and TT method require higher samples/wavelength than the SP and TP method for the error due to the EBC to be less than the error due to the IBC. As a result, the matrix size and computing time required for the EBC error to be less than the IBC error would be higher when the SS, ST, TS and TT method is used compared to the SP and TP method.

The TM scattering from hollow dielectric cylinder with typical outer and inner radius $b = (0.0819*2/\pi)$ m and $a = (0.0819*2*0.6/\pi)$ m is of smaller size and with typical outer and inner radius $b = (0.0819*2*2/\pi)$ m and $a = (0.0819*2*2*0.6/\pi)$ m is of larger size, in dielectric media with $\varepsilon_r = 54.2\text{-}j61.3$ (Yifen, et al., 2003) and $\varepsilon_r = 75.7\text{-}j67.1$ at 915 MHz are considered (Ikediala et al., 2002). The samples per wavelength of 50, 60, 70, 80 and 90 samples/ λ_0 where λ_0 is the free space wavelength corresponds to the MoM impedance matrix size of 160 by 160, 192 by 192, 224 by 224, 256 by 256 and 288 by 288 respectively for the smaller size object whereas for the larger size object this corresponds to the impedance matrix size of 320 by 320, 384 by 384, 448 by 448, 512 by 512 and 576 by 576 respectively. For the smaller size object, the impedance matrix size of 160 by 160, 192 by 192, 224 by 224, 256 by 256 and 288 by 288 corresponds to 25600, 36864, 50176, 65536 and 82944 matrix elements respectively. For the larger size object, the impedance matrix size of 320 by 320, 384 by 384, 448 by 448, 512 by 512 and 576 by 576 corresponds to 102400, 147456, 200704, 262144 and 331776 matrix elements respectively. The variation of outer layer magnetic current density mean relative error with samples per wavelength is tabulated in Table 13, 14, 15 and 16.

TABLE 13: Mean relative error for hollow dielectric cylinder with $\varepsilon_r = 54.2 - j61.3$ using
Gauss quadrature with smaller size

n	Equation	SP	SS	ST	TP	TS	TT
50	EFIE	0.0074	0.0343	0.0343	0.0085	0.0356	0.0356
	MFIE	0.0088	0.0373	0.0373	0.0077	0.0362	0.036
	PMCHW	0.0086	0.0404	0.0404	0.0076	0.0394	0.0392
	Muller	0.0249	0.1739	0.174	0.026	0.1757	0.1754
60	EFIE	0.0046	0.0215	0.0215	0.0054	0.0224	0.0224
	MFIE	0.0062	0.0242	0.0242	0.0054	0.0234	0.0233
	PMCHW	0.0058	0.0261	0.0261	0.0051	0.0254	0.0253
	Muller	0.0147	0.1052	0.1053	0.0155	0.1064	0.1062
70	EFIE	0.0031	0.0145	0.0145	0.0036	0.0151	0.0151
	MFIE	0.0046	0.0167	0.0167	0.004	0.0161	0.016
	PMCHW	0.0042	0.018	0.0179	0.0037	0.0174	0.0173
	Muller	0.0093	0.0692	0.0692	0.0099	0.07	0.0698
80	EFIE	0.0022	0.0102	0.0102	0.0026	0.0107	0.0107
	MFIE	0.0036	0.0121	0.0121	0.0032	0.0117	0.0116
	PMCHW	0.0032	0.0129	0.0129	0.0028	0.0125	0.0124
	Muller	0.0062	0.0481	0.0481	0.0066	0.0488	0.0486
90	EFIE	0.0016	0.0075	0.0075	0.0019	0.0079	0.0079
	MFIE	0.0029	0.0091	0.0091	0.0026	0.0087	0.0087
	PMCHW	0.0025	0.0097	0.0097	0.0022	0.0093	0.0093
	Muller	0.0043	0.035	0.035	0.0046	0.0355	0.0354

TABLE 14: Mean relative error for hollow dielectric cylinder with $\varepsilon_r = 54.2 - j61.3$ using
Gauss quadrature with larger size

n	Equation	SP	SS	ST	TP	TS	TT
50	EFIE	0.0064	0.0364	0.0364	0.0076	0.0377	0.0377
	MFIE	0.0098	0.0354	0.0353	0.0087	0.0342	0.0341
	PMCHW	0.0064	0.0352	0.0352	0.0054	0.0341	0.0341
	Muller	0.0514	0.35	0.35	0.0523	0.3513	0.3514
60	EFIE	0.0039	0.0228	0.0228	0.0047	0.0237	0.0237
	MFIE	0.0072	0.023	0.0229	0.0064	0.0221	0.0221
	PMCHW	0.0042	0.0226	0.0226	0.0035	0.0218	0.0218
	Muller	0.0307	0.2148	0.2148	0.0313	0.2156	0.2157
70	EFIE	0.0025	0.0153	0.0153	0.0031	0.016	0.016
	MFIE	0.0056	0.0159	0.0159	0.0051	0.0152	0.0152
	PMCHW	0.0029	0.0154	0.0154	0.0024	0.0148	0.0148
	Muller	0.0197	0.142	0.142	0.0201	0.1426	0.1426
80	EFIE	0.0017	0.0108	0.0108	0.0022	0.0113	0.0113
	MFIE	0.0046	0.0116	0.0115	0.0042	0.0111	0.011
	PMCHW	0.0022	0.011	0.011	0.0018	0.0106	0.0106
	Muller	0.0133	0.0992	0.0992	0.0136	0.0996	0.0996
90	EFIE	0.0013	0.0079	0.0079	0.0016	0.0083	0.0083
	MFIE	0.0039	0.0087	0.0087	0.0035	0.0084	0.0083
	PMCHW	0.0017	0.0082	0.0082	0.0014	0.0078	0.0078
	Muller	0.0093	0.0722	0.0722	0.0095	0.0725	0.0725

TABLE 15: Mean relative error for hollow dielectric cylinder with $\varepsilon_r = 75.7 - j67.1$ using Gauss quadrature with smaller size

n	Equation	SP	SS	ST	TP	TS	TT
50	EFIE	0.0076	0.0442	0.0442	0.0088	0.0456	0.0456
	MFIE	0.0116	0.0513	0.0512	0.0104	0.0502	0.05
	PMCHW	0.0113	0.0532	0.0532	0.0101	0.0521	0.0519
	Muller	0.03	0.2252	0.2252	0.0313	0.2271	0.2268
60	EFIE	0.0046	0.0277	0.0277	0.0054	0.0287	0.0287
	MFIE	0.0079	0.0334	0.0333	0.0071	0.0326	0.0325
	PMCHW	0.0076	0.0346	0.0345	0.0068	0.0338	0.0337
	Muller	0.0177	0.1348	0.1348	0.0185	0.136	0.1358
70	EFIE	0.003	0.0186	0.0186	0.0036	0.0193	0.0193
	MFIE	0.0058	0.023	0.023	0.0052	0.0225	0.0224
	PMCHW	0.0054	0.0238	0.0238	0.0048	0.0232	0.0231
	Muller	0.0111	0.0881	0.0881	0.0117	0.0889	0.0888
80	EFIE	0.0021	0.0131	0.0131	0.0025	0.0136	0.0136
	MFIE	0.0045	0.0166	0.0166	0.004	0.0162	0.0161
	PMCHW	0.0041	0.0172	0.0171	0.0036	0.0167	0.0166
	Muller	0.0073	0.0611	0.0611	0.0078	0.0617	0.0617
90	EFIE	0.0015	0.0095	0.0095	0.0018	0.01	0.01
	MFIE	0.0036	0.0125	0.0125	0.0032	0.0121	0.0121
	PMCHW	0.0032	0.0128	0.0128	0.0028	0.0125	0.0124
	Muller	0.005	0.0443	0.0443	0.0054	0.0448	0.0447

TABLE 16: Mean relative error for hollow dielectric cylinder with $\varepsilon_r = 75.7 - j67.1$ using Gauss quadrature with larger size

n	Equation	SP	SS	ST	TP	TS	TT
50	EFIE	0.0081	0.0485	0.0485	0.0095	0.0498	0.0498
	MFIE	0.0118	0.0465	0.0464	0.0106	0.0452	0.0452
	PMCHW	0.0084	0.046	0.046	0.0073	0.0449	0.0449
	Muller	0.075	0.5207	0.5208	0.076	0.5223	0.5225
60	EFIE	0.0049	0.0305	0.0305	0.0058	0.0314	0.0314
	MFIE	0.0084	0.0302	0.0302	0.0076	0.0293	0.0293
	PMCHW	0.0054	0.0296	0.0296	0.0046	0.0288	0.0288
	Muller	0.0448	0.317	0.317	0.0455	0.3179	0.318
70	EFIE	0.0032	0.0205	0.0205	0.0038	0.0212	0.0212
	MFIE	0.0064	0.0209	0.0209	0.0059	0.0202	0.0202
	PMCHW	0.0038	0.0203	0.0203	0.0032	0.0197	0.0197
	Muller	0.0288	0.2082	0.2082	0.0293	0.2088	0.2089
80	EFIE	0.0022	0.0145	0.0145	0.0027	0.015	0.015
	MFIE	0.0052	0.0151	0.0151	0.0047	0.0146	0.0146
	PMCHW	0.0028	0.0145	0.0145	0.0023	0.014	0.014
	Muller	0.0195	0.1448	0.1448	0.0198	0.1452	0.1452
90	EFIE	0.0015	0.0106	0.0106	0.0019	0.011	0.011
	MFIE	0.0043	0.0114	0.0114	0.004	0.011	0.011
	PMCHW	0.0021	0.0108	0.0108	0.0018	0.0104	0.0104
	Muller	0.0137	0.1051	0.1051	0.014	0.1054	0.1054

For the high permittivity hollow dielectric cylinder, the different integral equations are governed by 2 surface electric current densities and 2 surface magnetic current densities on the outer and inner layer respectively. Therefore, 3 integral equations in the EFIE and MFIE and also 4 integral equations in the PMCHW and Muller integral equation is contaminated by the error due to the small argument approximation of the Hankel function. The inner layer surface current densities is affected by the error due to the small argument approximation of the Hankel function which is intensified by the high relative permittivity and this slows down the convergence of the outer layer surface current densities.

In addition to that, the outer layer surface current densities is also affected by the error due to the small argument approximation of the Hankel function that is intensified by the high relative permittivity and this also slows down the convergence of the outer layer surface current density. As a result, the mesh element size has to be small by taking a significantly large number of segmentation for the outer and inner layer of the hollow dielectric cylinder with larger size to minimize the error due to small argument approximation of the Hankel function. By increasing both the outer and inner radius of the high permittivity hollow dielectric cylinder, the impedance matrix size and therefore the number of impedance matrix elements utilised had to be increased to minimize the error of the numerical solution.

The numerical results imply that the larger the size of the hollow dielectric cylinder by increasing the magnitude of the inner and outer radius, the SP and TP method provide faster convergence than the SS, ST, TS and TT method with a higher difference in the number of matrix elements or matrix size between the SS, ST and SP method and also between TS, TT and TP method to achieve an error less than 0.01. When the size of the high permittivity hollow dielectric cylinder is smaller by having a smaller inner and outer radius, the SP and TP method still provide faster convergence than the SS, ST, TS and TT method with smaller difference in the number of matrix elements between SS, ST and SP method and also between TS, TT and TT method to achieve and error less than 0.01 is observed. This indicate that the efficiency of the numerical solution in terms of memory requirements denoted by the number of matrix elements or matrix size to achieve an error less than 0.01 for the SS, ST, TS and TT method would be significantly different than the SP and TP method as the size of the high permittivity object is increased.

It can be deduced that the amount of difference in the number of impedance matrix elements or matrix size between SS, ST and SP method and also between TS, TT and TP method to achieve an error less than 0.01 depends on the size of the high permittivity object. From the numerical experimentation, a larger difference in the efficiency in terms of the number of matrix elements or matrix size is observed between the SS, ST and SP method and also between the TS, TT and TP method to achieve an error less than 0.01 for larger size high permittivity object compared to the object with smaller size. When the size of the high permittivity object is smaller, this leads to a smaller difference in the efficiency in terms of impedance matrix size or number of impedance matrix elements between the SS, ST and SP method and also between the TS, TT and TP method to achieve an error less than 0.01. Higher difference in the number of matrix elements or matrix size in minimizing the error between the different basis and testing function denotes a higher difference in the memory usage in minimizing the error of the numerical solution.

6. CONCLUSION

Different basis and testing function is applied on different integral equations where different numerical implementation, boundary conditions and different sizes is considered. The convergence and accuracy of different integral equations using different testing function is compared when the integral equations are applied on two dimensional dielectric objects. Numerical results for the MoM surface integral equation using different basis and testing function on dielectric objects indicate that different computing technique and different boundary conditions can result in different convergence rate and different error contamination when different basis and testing function is used as the MoM impedance matrix size is reduced to save memory requirements and computing time.

REFERENCES

Ayyildiz, K. 2006. Surface Integral Solution of Chiral Loaded Waveguides of Arbitrary Cross Section, Ph.D Thesis, Sycrause University, US.

Beker, B., Umashankar, K. R. and Taflove, A. 1990. Electromagnetic Scattering by Arbitrarily Shaped Two-Dimensional Perfectly Conducting Objects Coated with Homogeneous Anisotropic Materials. *Electromagnetics*. **10**(4):387-406.

Bussey, H. E. and Richmond, J. H. 1975. Scattering by a Lossy Dielectric Circular Cylindrical Multilayer, Numerical Values. *IEEE Trans. Antennas Propagat.* **23**(5):723- 725.

Davis, C. P. and Warnick, K. F. 2004. Higher-Order Convergence With Low Order Discretisation of the 2D-MFIE. *IEEE Antennas Wireless Propagat. Letters.* **3**(1):355-358.

Davis, C. P. and Warnick, K. F. 2005. Error Analysis of 2-D MoM for MFIE/EFIE/CFIE based on the Circular Cylinder. *IEEE Trans. Antennas Propagat.* **53**(1):321-331.

Gibson, W. C. 2007. *The Method of Moments in Electromagnetics.* Boca Raton: Chapman and Hall/CRC.

Huddleston, P. L., Medgyesi–Mitschang, L. N. and Putnam, J. M. 1986 Combined Field Integral Equation Formulation for Scattering by Dielectrically Coated Conducting Bodies. *IEEE Trans. Antennas Propagat.* **34**(4):510-520.

Ikediala, J. N., Hansen, J. D., Tang, J., Drake, S. R. and Wang, S. 2002. Development of a saline water immersion technique with RF energy as a postharvest treatment against codling moth in cherries. *Postharvest Biology and Technology.* **24**(2):209-221.

Jin, J. M. 2010. *Theory and Computation of Electromagnetic Fields*. John Wiley and Sons.

Kishk, A. A. 1991. Electromagnetic Scattering from Composite Objects Using a Mixture of Exact and Impedance Boundary Conditions. *IEEE Trans. Antennas Propagat.* **39**(6):826-833.

Kishk, A. A., Glisson, A. W., Goggans, P. M. 1992. Scattering from Conductors Coated with Materials of Arbitrary Thickness. *IEEE Trans. Antennas Propagat.* **40**(1):108-112.

Peterson, A. F. 1994. Application of volume discretisation methods to oblique scattering from high contrast penetrable cylinders. *IEEE Trans. Microwave Theory and Techniques*. **42**(4):686-689.

Peterson, A. F., Ray, S. L. and Mittra, R. 1998. *Computational Methods for Electromagnetics*. New York: IEEE Press.

Yifen, W., Timothy, D. W., Juming, T. and Linnea, M. H. 2003. Dielectric properties of foods relevant to RF and microwave pasteurization and sterilization. *Journal of Food Engineering.* **57**:257–268.